# COMPARING ANTENNA SELECTION AND HYBRID PRECODING FOR MILLIMETER WAVE WIRELESS COMMUNICATIONS

*Erich Zöchmann, Stefan Schwarz, and Markus Rupp*

Christian Doppler Laboratory for Dependable Wireless Connectivity for the Society in Motion
Institute of Telecommunications, TU Wien, Austria
{ezoechma,sschwarz,mrupp}@nt.tuwien.ac.at

**ABSTRACT**

Due to the small wavelengths at millimetre wave frequencies, antenna arrays with dozens of elements fit easily even in hand-held devices. As RF chains are power hungry and costly, all-digital approaches are impractical and analogue-digital co-designs are likely to come. Common for all approaches is a dimensional reduction of the large MIMO channel. This study compares Antenna Selection (AS) and Hybrid Precoding (HP). In HP systems, channels are estimated employing a set of hybrid codebooks exploiting all antennas. For AS we propose a bistatic MIMO radar method to estimate the channel even with a reduced number of antennas, identical to the number of RF chains.

***Index Terms*—** mmWave Channel Estimation, 5G, MIMO radar, Bistatic Radar, Antenna Selection, Achievable Rate

## 1. INTRODUCTION

### 1.1. Importance and Prior Work

Next generation mobile communications will possibly employ the underutilized spectrum in the MilliMetre Wave (MMW) band. The authors of [1] predict a further evolution of existing LTE-Advanced systems in parallel to the development of new radio-access technologies [2–5], also operating at millimetre wave frequencies. The challenging propagation condition, due to higher diffraction and penetration losses, must be countered via beamforming [6].

Initial beamforming architectures will be less complex and the all-digital approach employed in the low GHz regime will likely not be applied at MMW frequencies because of high costs and high power consumptions of the numerous RF chains [7]. To enable spatial multiplexing much research focused on Hybrid Precoding (HP), where part of the beamforming is performed by analogue phase shifters [8–11].

The origins of HP can be traced back to [12] and the Antenna Selection (AS) papers [13, 14]. The authors of [13] proposed to embed an analogue FFT prior to the RF chains, for spatially correlated channels. MMW channels are commonly modelled with limited, dominant scattering objects, constructing distinct propagation paths from transmit (TX) to receive (RX) site. This assumption and the mostly employed $\frac{\lambda}{2}$ spaced antenna arrays lead to spatially correlated channels, justifying the interest in HP.

This work has been funded by A1 Telekom Austria AG and the Institute of Telecommunications, TU Wien. The financial support by the Austrian Federal Ministry of Science, Research and Economy and the National Foundation for Research, Technology and Development is gratefully acknowledged.

Although, research on HP produced quite promising results, some limitations are commonly not taken into account. HP architectures need typically more power than AS schemes, as analysed in [15, 16]. The phase shift networks (PSNs) employed with HP have much higher insertion loss than switches [17], which can add 6 dB compared to switches when applied on both sites. Furthermore, high resolution analogue phase shifters (4-5 bits) are currently state of research [18–21].

### 1.2. Contributions

This paper shows the performance loss of HP caused by limited PSN resolution and the additional insertion loss of the analogue PSN. The substantial drop of the achievable rates of HP is mainly caused by a decreased Channel Estimation (CE) performance. A new CE approach based on bistatic MIMO radar [22–24] is proposed. Orthogonal waveforms at the transmitter enable good estimation of the commonly used geometric channel model [25] already with fairly few antennas. The thereby obtained channel estimate renders AS possible, since only a limited number of receiver chains / antennas are available in AS schemes. Our proposed MIMO radar CE method applying AS [26, 27] is then compared to HP.

### 1.3. Outline and Notation

Section 2 reviews HP, especially the assumed channel model and its estimation. Section 3 reviews AS and shows that estimating an underlying sparse multipath channel can be considered as bistatic MIMO radar problem. In Section 4 we compare both approaches in terms of spectral efficiency before we conclude in Section 5.

Throughout the paper matrices are denoted by bold upper-case letters such as $\boldsymbol{Y}$ and vectors by bold lower-case letters such as $\boldsymbol{y}$. The superscripts $(\cdot)^*$, $(\cdot)^T$ and $(\cdot)^H$ express conjugate complex, transposition and conjugate transposition, respectively. The Kronecker product is denoted by $\otimes$. Whenever we write a bold faced uppercase letter after introducing its lowercase version we implicitly assume that we stack in time, e.g., $\boldsymbol{Y} = [\boldsymbol{y}_1, \boldsymbol{y}_2, \dots]$.

## 2. HYBRID PRECODING

### 2.1. HP System Model

Measurement campaigns conducted at MMW bands [28–31] support the idea of a sparse multipath channel [25], i.e.,

$$\boldsymbol{H} = \sqrt{\frac{N_t N_r}{\rho}} \sum_{p=1}^{P} \alpha_p \boldsymbol{a}_r(\phi_{r,p}) \boldsymbol{a}_t(\phi_{t,p})^H, \quad \boldsymbol{H} \in \mathbb{C}^{N_r \times N_t}, \tag{1}$$

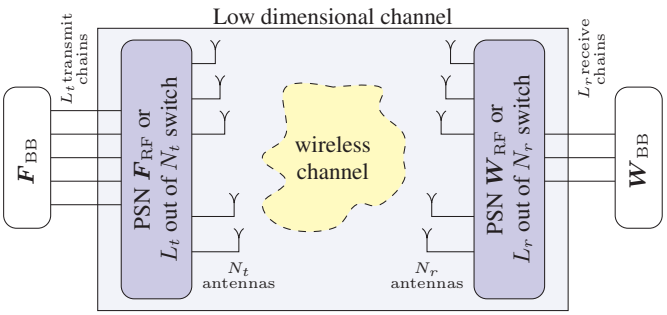


**Fig. 1**: Generic system model for HP and AS.

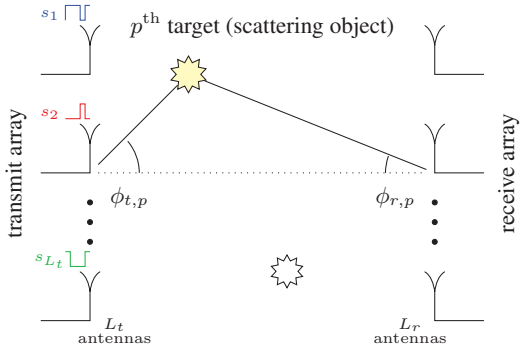


**Fig. 2**: A Bistatic MIMO radar scenario with two scattering objects.

where $N_t, N_r$ are the number of transmit and receive antennas, $\rho$ is the average path loss, $P$ is the number of paths with respective gains $\alpha_p$. The number of MultiPath Components (MPC) $P \ll \min(N_r, N_t)$ is assumed to be rather low for MMW channels [29]. The ideal steering vectors of a Uniform Linear Array (ULA) $\boldsymbol{a}_r(\phi_{r,p}) \in \mathbb{C}^{N_r}$, $\boldsymbol{a}_t(\phi_{t,p}) \in \mathbb{C}^{N_t}$ belong to the transmitter's Angle-of-Departure (AOD) $\phi_{t,p}$ and the receiver's Angle-of-Arrival (AOA) $\phi_{r,p}$, respectively[1].

HP employs digital baseband precoders $\boldsymbol{F}_{\mathrm{BB}}, \boldsymbol{W}_{\mathrm{BB}}$ operating on a reduced size channel matrix of size $\mathbb{C}^{L_r \times L_t}$, where the size-reduction was carried out by an analogue PSN $\boldsymbol{F}_{\mathrm{RF}}, \boldsymbol{W}_{\mathrm{RF}}$, cf., Fig 1. Such an approach is generally suboptimal in terms of spectral efficiency as fewer spatial streams can be supported. Under the assumption of the sparse multipath channel in Eq. (1) the full-size channel exhibits already a low rank structure and size-reduction may come without significant spectral efficiency loss.

### 2.2. Channel Estimation with PSN

Channel estimation with PSNs [9] is performed by applying consecutive transmit precoders $\boldsymbol{f}_i = \boldsymbol{F}_{\mathrm{RF}} \boldsymbol{f}_{i,\mathrm{BB}},\ i = 1, \ldots, M_t$ for each of the fixed receive precoders $\boldsymbol{w}_j = \boldsymbol{W}_{\mathrm{RF}} \boldsymbol{w}_{j,\mathrm{BB}},\ j = 1, \ldots, M_r$. Overall $M = M_t M_r$ measurement steps are needed. Assuming all training symbols equal and of power $\sigma_s^2$ and stacking all $\boldsymbol{f}$, $\boldsymbol{w}$, the receive matrix can be written as

$$\boldsymbol{Y} = \sigma_s \boldsymbol{W}^H \boldsymbol{H} \boldsymbol{F} + \boldsymbol{N}\,, \tag{2}$$

with $\boldsymbol{N} \in \mathbb{C}^{M_t \times M_r}$ denoting temporally and spatially white, circularly symmetric Gaussian noise of variance $\sigma_n^2$. The vectorized estimation problem can be solved by a discretization in the angular domain

$$\begin{aligned} \mathrm{vec}(\boldsymbol{Y}) &= \sigma_s \left(\boldsymbol{F}^T \otimes \boldsymbol{W}^H\right) \sum_{p=1}^{P} \alpha_p \boldsymbol{a}_r(\phi_{r,p}) \otimes \boldsymbol{a}_t^*(\phi_{t,p}) + \boldsymbol{n} \\ &= \sigma_s \left(\boldsymbol{F}^T \otimes \boldsymbol{W}^H\right) \boldsymbol{A}\boldsymbol{\alpha} + \boldsymbol{n} \qquad (3) \\ &\approx \sigma_s \left(\boldsymbol{F}^T \otimes \boldsymbol{W}^H\right) \boldsymbol{A}_D \boldsymbol{z} + \boldsymbol{n} = \boldsymbol{\Phi}\boldsymbol{z} + \boldsymbol{n}\,. \qquad (4) \end{aligned}$$

Discretizing the angular domain with $M_D$ samples, i.e., enlarging $\boldsymbol{A}$ to $\boldsymbol{A}_D$ with steering vectors for $\phi = 0, \frac{2\pi}{M_D}, \ldots, \frac{(M_D-1)2\pi}{M_D}$ to solve for a path gain vector $z \in \mathbb{C}^{M_D^2}$, yields a measurement matrix $\boldsymbol{\Phi}$ of size $M_t M_r \times M_D^2$. For sufficient measurements $M = M_t M_r$ and suitable angular sampling compressive sensing (CS) methods are readily applicable [32]. In our simulations we included the algorithm proposed in [9], which relies on a smart multi-stage code-book design for $\boldsymbol{F}$ and $\boldsymbol{W}$ for fast CE.

[1] In this work, we consider only 1D arrays without the elevation domain.

## 3. ANTENNA SELECTION

### 3.1. AS System Model

AS tries to optimally select the best set of $L_t$ transmit and $L_r$ receive antennas to maximize the systems capacity [26]. This non-convex problem implicates an exhaustive search among $\binom{N_t}{L_t}\binom{N_r}{L_r}$ possible subsets. The authors of [26] propose to decouple the joint search and to apply the fast subset selection algorithm from [27] at the transmitter and receiver individually[2].

For the purpose of channel estimation we do not change the selected antennas adaptively and select $L_t$ and $L_r$ consecutive antenna elements at TX and RX to apply the channel estimation algorithm described in Section 3.2[3].

### 3.2. Channel Estimation by Bistatic MIMO Radar Algorithms

In contrast to phased-array radar, MIMO radar [33] transmits different probing signals on its antennas. The number of targets identifiable by MIMO radars scales linearly with the number of transmit antennas [34]. The covariance matrix of the probing signal is subject to design and can be used to maximize power around expected target positions [35]. In our contribution we do not use this feature; the signal's covariance matrix always equals identity and is never adapted.

The receive signal at time $k$ of a bistatic MIMO radar [22–24], as depicted in Fig. 2, with $L_t$ transmit and $L_r$ receive antennas can be described via

$$\boldsymbol{r}(k) = \sum_{p=1}^{P} \alpha_p \boldsymbol{a}_r'(\phi_{r,p}) \boldsymbol{a}_t'(\phi_{t,p})^T \boldsymbol{s}(k) + \boldsymbol{n}\,, \tag{5}$$

where $\alpha_p$ is the radar cross section of the $p^{\mathrm{th}}$ target. The transmit vector $\boldsymbol{s}(k) = (s_1(k), \ldots, s_{L_t}(k))^T$ consists of time orthogonal sequences $s_p(k)$. Note, that the steering vectors are of reduced dimension now ($\boldsymbol{a}_t' \in \mathbb{C}^{L_t}$, $\boldsymbol{a}_r' \in \mathbb{C}^{L_r}$), resembling a sub-ULA. By

[2] We selected the transmit subset first as [26] has shown that the order of subset selection plays a minor role.

[3] Changing the antenna subset, used for channel estimation, over time might yield some gains. We do not consider this within this contribution.

**Table 1**: Simulation Parameters

| Parameter | Value | Parameter | Value |
|---|---|---|---|
| $N_t$ | 64 | $L_t$ | 16 |
| $N_r$ | 16 | $L_r$ | 8 |
| PSN bits | 4-6 | $M_D$ | 192 |
| $K = M$ | 108 | PSN add. insertion loss | 3 dB |
| TX-RX dist. | 50 m | Pathloss exponent | 3 |
| $\sigma_s^2$ | 37 dBm | Carrier frequency | 28 GHz |
| Channel BW | 100 MHz | Noise figure | 0 dB |

assuming the target constant across time and matched filtering with $\boldsymbol{S}$ after $K \geq N_t$ time steps we arrive at

$$\boldsymbol{Y} = (\boldsymbol{R} + \boldsymbol{N})\boldsymbol{S}^H = \left( \sum_{p=1}^{P} \alpha_p \boldsymbol{a}_r'(\phi_{r,p}) \boldsymbol{a}_t'(\phi_{t,p})^T \right) \underbrace{\boldsymbol{S}\boldsymbol{S}^H}_{\boldsymbol{I}} + \boldsymbol{N}' \, . \tag{6}$$

Performing vectorization we obtain

$$\mathrm{vec}(\boldsymbol{Y}) = \sum_{p=1}^{P} \alpha_p \boldsymbol{a}_r'(\phi_{r,p}) \otimes \boldsymbol{a}_t'(\phi_{t,p}) + \mathrm{vec}(\boldsymbol{N}') = \boldsymbol{A}'\boldsymbol{\alpha} + \boldsymbol{n}' \, . \tag{7}$$

Based on Equation (7), subspace methods such as MUSIC and ESPRIT, or computationally more complex methods such as ML and CS can be applied; in this contribution we use 2D-MUSIC and its solution is given by

$$(\hat{\boldsymbol{\phi}}_t, \hat{\boldsymbol{\phi}}_r) = \underset{\phi_t, \phi_r}{\mathrm{argmax}} \left( \boldsymbol{a}_r'(\phi_r) \otimes \boldsymbol{a}_t'(\phi_t) \right) \boldsymbol{E}_n \boldsymbol{E}_n^H \left( \boldsymbol{a}_r'(\phi_r) \otimes \boldsymbol{a}_t'(\phi_t) \right), \tag{8}$$

where $\boldsymbol{E}_n$ contains $L_t L_r - P$ eigenvectors that span the noise subspace. We apply the computationally efficient 2D-MUSIC algorithm introduced in [23], which exploits the Kronecker structure in Eq. (8).

## 4. SIMULATIONS

The simulation set-up is based on that of [9]. The key features are summarized in Table 1. A very early work [28] determined the multipath components of measured 40 GHz indoor channels. Those vary depending on the type of antennas and obstructions used. LOS channels with horn antennas where found to have a low number of multipath components (MPCs) and are modelled with thre MPCs. Obstructed NLOS channels are modelled with six MPCs.

The Signal-to-Noise-Ratio (SNR) is given as ratio of the average receive power (without beamforming) and the noise floor at room temperature. To focus on the effect of erroneous HP or AS, the channel was first estimated by the corresponding method at roughly -10 dB SNR and thereof the optimal HP and AS parameters are deduced. Those are applied on the perfectly known channel (as generated) and spectral efficiency is calculated there from. The work of [36] has already shown that erroneous selection of antenna elements do not lead to large performance drops, unless the channel estimation error remains small.

For Figs. 3-6 we fix three scattering objects and show a scatterplot of the AOA / AOD estimate for 10 different noise realisations. The virtual channel [37] is put under the scatterplot to visually inspect the CE performance. The CE performance drop of beam-searching algorithms is studied applying the opportunistic case of exhaustive beam search, i.e., applying the narrowest possible beamformer to all directions[4].

[4]We show the opportunistic case to exclude the algorithm of [9] as major error source.

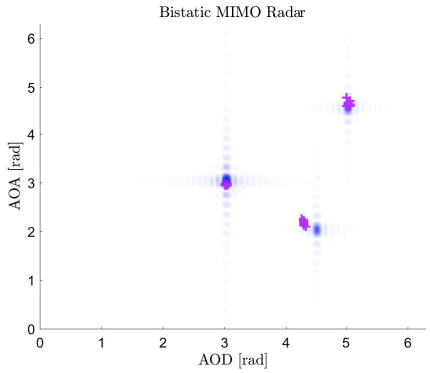


**Fig. 3**: AOA / AOD for bistatic MIMO radar CE.

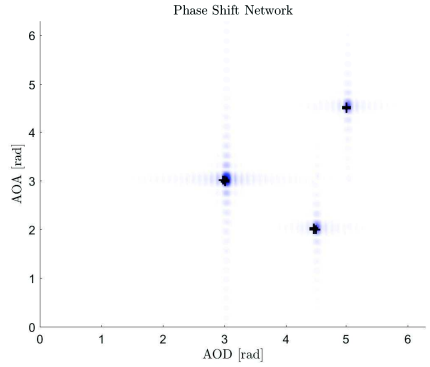


**Fig. 4**: AOA / AOD for exhaustive beam search with 6 bit PSN.

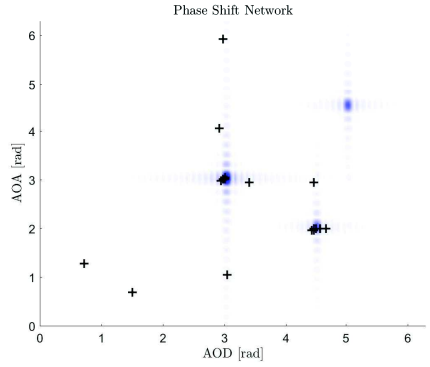


**Fig. 5**: AOA / AOD for exhaustive beam search with 5 bit PSN.

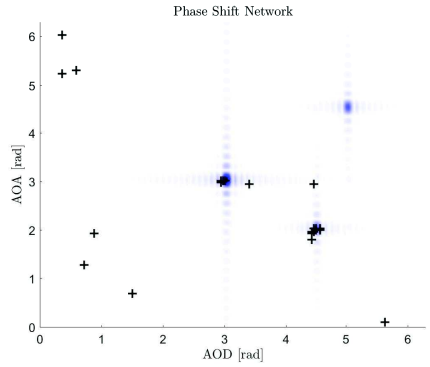


**Fig. 6**: AOA / AOD for exhaustive beam search with 5 bit PSN including additional insertion loss.

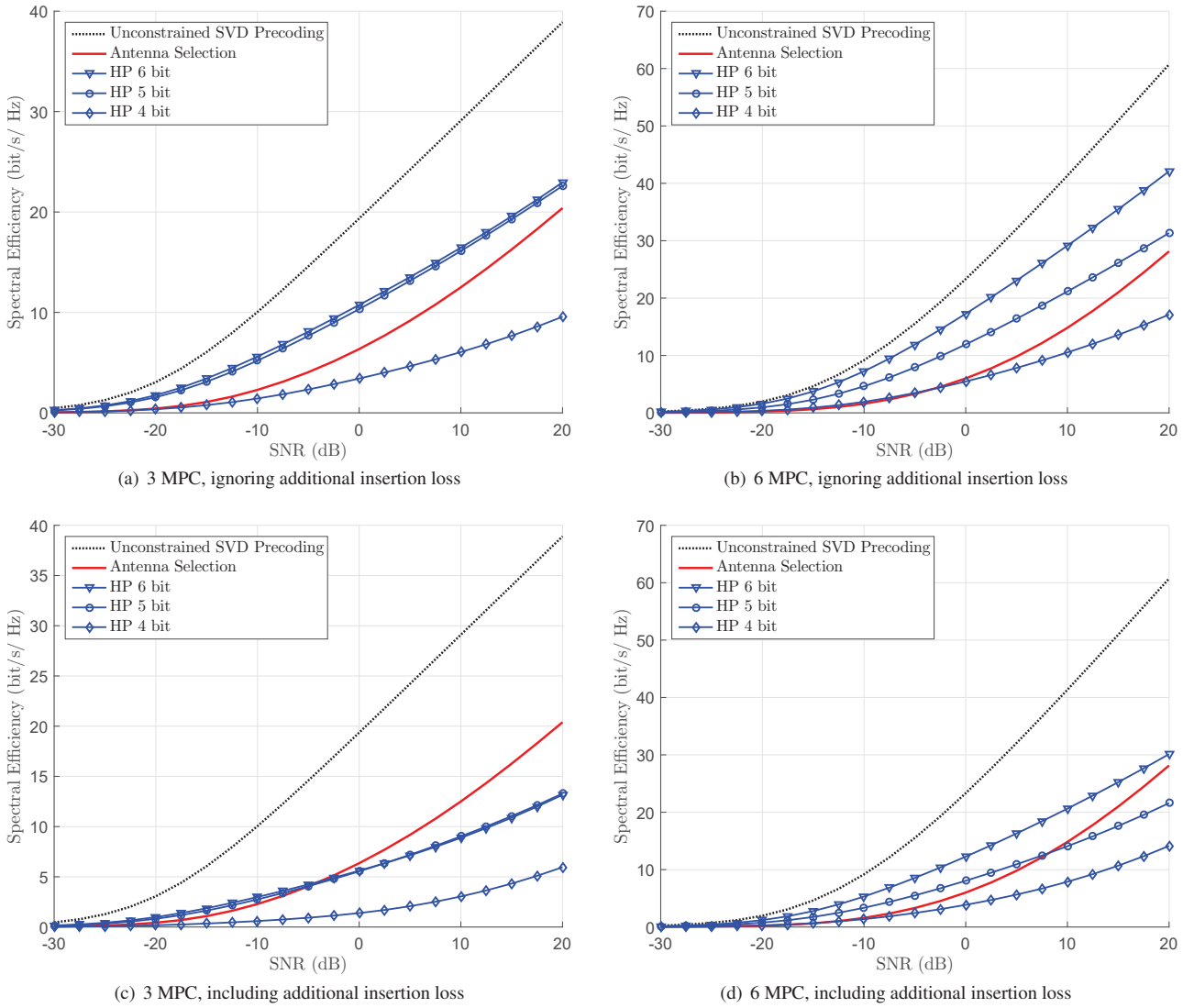


(a) 3 MPC, ignoring additional insertion loss

(b) 6 MPC, ignoring additional insertion loss

(c) 3 MPC, including additional insertion loss

(d) 6 MPC, including additional insertion loss

**Fig. 7**: Spectral efficiency of HP for various PSN resolutions and AS for a channel with three and six multipath components ignoring and including additional insertion loss of the PSN.

As exhaustive beam search demands a very long channel coherence time, we use the orders of magnitude faster adaptive multi-stage codebook search of [9] to compare achievable rates[5]. Simulations show that the influence of the PSN resolution depends on the number of MPCs in the channel. For a very low number of MPCs, which might be the case for LOS channels, the effect becomes visual for a resolution of $\leq 4$ bits, cf., Fig. 7 (a) for results still ignoring additional insertion loss. Surprisingly, the performance of the fast antenna selection scheme together with bistatic MIMO radar channel estimation performs already quite close to HP. Figure 7 (b) reveals a performance gap for channels featuring more MPCs; the gap is particularly increasing for higher PSN resolution. Insertion loss favours the AS approach as the impact on HP is quite severe, cf. Figs 7 (c) and 7 (d). The curves for HP are not only shifted by 6 dB, they also flat out due to a poorer channel estimation.

## 5. CONCLUSION

We have shown a new approach for channel estimation of sparse multipath channels, which are reported for millimetre wave wireless communications [29]. This new approach is well suited for antenna selection architectures.

A comparison with hybrid precoding based schemes based on channel estimation with analogue/digital co-designed codebooks was conducted. Antenna selection architectures can perform close to hybrid precoding schemes and might be especially useful for hand-held devices, due to their simpler RF and the reduced power consumption of switches compared to analogue phase shifters.

[5]The increased speed comes again at performance expense.

## 6. REFERENCES


[1] E. Dahlman, G. Mildh, S. Parkvall, J. Peisa, J. Sachs, Y. Selen, and J. Skold, "5G wireless access: requirements and realization," *IEEE Communications Magazine*, vol. 52, no. 12, pp. 42–47, December 2014.

[2] R. Nissel and M. Rupp, "On pilot-symbol aided channel estimation in FBMC-OQAM," in *IEEE International Conference on Acoustics, Speech and Signal Processing (ICASSP)*, Shanghai, China, mar 2016.

[3] R. Nissel, S. Caban, and M. Rupp, "Experimental evaluation of FBMC-OQAM channel estimation based on multiple auxiliary symbols," in *IEEE 9th Sensor Array and Multichannel Signal Processing Workshop (SAM 2016)*, Rio de Janeiro, Brazil, Jul. 2016.

[4] R. Nissel and M. Rupp, "Dynamic spectrum allocation in cognitive radio: Throughput calculations," in *IEEE International Black Sea Conference on Communications and Networking (BlackSeaCom)*, Varna, Bulgaria, jun 2016.

[5] S. Schwarz and M. Rupp, "Society in motion: Challenges for LTE and beyond mobile communications," *IEEE Communications Magazine, Feature Topic: LTE Evolution*, vol. 54, no. 5, 2016.

[6] Z. Pi and F. Khan, "An introduction to millimeter-wave mobile broadband systems," *IEEE Communications Magazine*, vol. 49, no. 6, pp. 101–107, 2011.

[7] S. Sun, T. S. Rappaport, R. W. Heath, A. Nix, and S. Rangan, "MIMO for millimeter-wave wireless communications: Beamforming, spatial multiplexing, or both?" *IEEE Communications Magazine*, vol. 52, no. 12, pp. 110–121, 2014.

[8] O. El Ayach, S. Rajagopal, S. Abu-Surra, Z. Pi, and R. W. Heath, "Spatially sparse precoding in millimeter wave MIMO systems," *IEEE Transactions on Wireless Communications*, vol. 13, no. 3, pp. 1499–1513, 2014.

[9] A. Alkhateeb, O. El Ayach, G. Leus, and R. W. Heath, "Channel estimation and hybrid precoding for millimeter wave cellular systems," *IEEE Journal of Selected Topics in Signal Processing*, vol. 8, no. 5, pp. 831–846, 2014.

[10] S.-F. Chuang, W.-R. Wu, and Y.-T. Liu, "High-resolution AoA estimation for hybrid antenna arrays," *IEEE Transactions on Antennas and Propagation*, vol. 63, no. 7, pp. 2955–2968, July 2015.

[11] S. Han, I. Chih-Lin, Z. Xu, and C. Rowell, "Large-scale antenna systems with hybrid analog and digital beamforming for millimeter wave 5G," *IEEE Communications Magazine*, vol. 53, no. 1, pp. 186–194, 2015.

[12] V. Venkateswaran and A.-J. Van der Veen, "Analog beamforming in MIMO communications with phase shift networks and online channel estimation," *IEEE Transactions on Signal Processing*, vol. 58, no. 8, pp. 4131–4143, 2010.

[13] A. F. Molisch and X. Zhang, "FFT-based hybrid antenna selection schemes for spatially correlated MIMO channels," *IEEE Communications Letters*, vol. 8, no. 1, pp. 36–38, 2004.

[14] X. Zhang, A. F. Molisch, and S.-Y. Kung, "Variable-phase-shift-based RF-baseband codesign for MIMO antenna selection," *IEEE Transactions on Signal Processing*, vol. 53, no. 11, pp. 4091–4103, 2005.

[15] R. Mendez-Rial, C. Rusu, A. Alkhateeb, N. Gozalez-Prelcic, and R. W. Heath Jr, "Channel estimation and hybrid combining for mmWave: Phase shifters or switches?" in *Information Theory and Applications Workshop (ITA)*, 2015.

[16] R. Mendez-Rial, C. Rusu, N. Gonzalez-Prelcic, A. Alkhateeb, and R. Heath, "Hybrid MIMO architectures for millimeter wave communications: Phase shifters or switches?" *IEEE Access*, vol. PP, no. 99, pp. 1–1, 2016.

[17] A. S. Nagra, R. York *et al.*, "Distributed analog phase shifters with low insertion loss," *IEEE Transactions on Microwave Theory and Techniques*, vol. 47, no. 9, pp. 1705–1711, 1999.

[18] Y. Yu, P. Baltus, A. de Graauw, E. van der Heijden, C. Vaucher, and A. van Roermund, "A 60 GHz phase shifter integrated with LNA and PA in 65 nm CMOS for phased array systems," *IEEE Journal of Solid-State Circuits*, vol. 45, no. 9, pp. 1697–1709, Sept 2010.

[19] W.-T. Li, Y.-C. Chiang, J.-H. Tsai, H.-Y. Yang, J.-H. Cheng, and T.-W. Huang, "60-GHz 5-bit phase shifter with integrated VGA phase-error compensation," *IEEE Transactions on Microwave Theory and Techniques*, vol. 61, no. 3, pp. 1224–1235, March 2013.

[20] M. Uzunkol and G. Rebeiz, "A 65 GHz LNA/phase shifter with 4.3 db NF using 45 nm CMOS SOI," *IEEE Microwave and Wireless Components Letters*, vol. 22, no. 10, pp. 530–532, Oct 2012.

[21] C. Zhou, L. Zhang, Y. Wang, Z. Yu, and H. Qian, "A 4-bit CMOS phase shifter for millimeter-wave phased arrays," *Analog Integrated Circuits and Signal Processing*, vol. 79, no. 3, pp. 461–468, 2014.

[22] H. Yan, J. Li, and G. Liao, "Multitarget identification and localization using bistatic MIMO radar systems," *EURASIP J. Adv. Signal Process*, pp. 48:1—-48:8, 2008.

[23] R. Xie, Z. Liu, and J.-x. Wu, "Direction finding with automatic pairing for bistatic MIMO radar," *Signal Processing*, vol. 92, no. 1, pp. 198–203, 2012.

[24] B. Tang, J. Tang, Y. Zhang, and Z. Zheng, "Maximum likelihood estimation of DOD and DOA for bistatic MIMO radar," *Signal Processing*, vol. 93, no. 5, pp. 1349–1357, 2013.

[25] A. Sayeed and V. Raghavan, "Maximizing MIMO capacity in sparse multipath with reconfigurable antenna arrays," *IEEE Journal of Selected Topics in Signal Processing*, vol. 1, no. 1, pp. 156–166, June 2007.

[26] S. Sanayei and a. Nosratinia, "Capacity maximizing algorithms for joint transmit-receive antenna selection," in *Conference Record of the Thirty-Eighth Asilomar Conference on Signals, Systems and Computers, 2004.*, 2004.

[27] M. Gharavi-Alkhansari and A. B. Gershman, "Fast antenna subset selection in MIMO systems," *IEEE Transactions on Signal Processing*, vol. 52, pp. 339–347, 2004.

[28] P. L. C. Cheong, "Multipath component estimation for indoor radio channels," in *Global Telecommunications Conference*, vol. 2. IEEE, 1996, pp. 1177–1181.

[29] T. S. Rappaport, S. Sun, R. Mayzus, H. Zhao, Y. Azar, K. Wang, G. N. Wong, J. K. Schulz, M. Samimi, and F. Gutierrez, "Millimeter wave mobile communications for 5G cellular: It will work!" *IEEE Access*, vol. 1, pp. 335–349, 2013.

[30] E. Zöchmann, M. Lerch, S. Caban, R. Langwieser, C. F. Mecklenbräuker, and M. Rupp, "Directional evaluation of receive power, Rician K-factor and RMS delay spread obtained from power measurements of 60 GHz indoor channels," in *IEEE-APS Topical Conference on Antennas and Propagation in Wireless Communications (APWC 2016)*, Cairns, Australia, Sep. 2016.

[31] E. Zöchmann, S. Caban, M. Lerch, and M. Rupp, "Resolving the angular profile of 60 GHz wireless channels by delay-Doppler measurements," in *IEEE 9th Sensor Array and Multichannel Signal Processing Workshop (SAM 2016)*, Rio de Janeiro, Brazil, Jul. 2016.

[32] D. Malioutov, M. Cetin, and A. Willsky, "A sparse signal reconstruction perspective for source localization with sensor arrays," *IEEE Transactions on Signal Processing*, vol. 53, no. 8, pp. 3010–3022, Aug 2005.

[33] J. Li and P. Stoica, "MIMO radar with colocated antennas," *IEEE Signal Processing Magazine*, vol. 24, no. 5, pp. 106–114, 2007.

[34] J. Li, P. Stoica, L. Xu, and W. Roberts, "On parameter identifiability of MIMO radar," *IEEE Signal Processing Letters*, vol. 14, no. 12, pp. 968–971, 2007.

[35] P. Stoica, J. Li, and Y. Xie, "On probing signal design for MIMO radar," *IEEE Transactions on Signal Processing*, vol. 55, no. 8, pp. 4151–4161, 2007.

[36] A. F. Molisch and M. Z. Win, "MIMO systems with antenna selection," *IEEE Microwave Magazine*, vol. 5, no. 1, pp. 46–56, 2004.

[37] A. M. Sayeed, "Deconstructing multiantenna fading channels," *Signal Processing, IEEE Transactions on*, vol. 50, no. 10, pp. 2563–2579, 2002.